© IWA Publishing 2020
652

Water Practice & Technology Vol 15 No 3
doi: 10.2166/wpt.2020.048

Use of a self-rotating nozzle for more efficient flash purification of dirty water

Hery Sonawan* and Kiki Aprillianto

Teknik Mesin, Universitas Pasundan Bandung, Jalan Setiabudi No. 193 Bandung, Jawa Barat, Indonesia

*Corresponding author. E-mail: herysonawan@unpas.ac.id

Abstract

An efficient flash-purification system has been developed using a self-rotating nozzle powered by the feed-water flow. Where an electrically-powered, rotating nozzle distributes water droplets evenly in a flashing chamber to increase the evaporation rate, a self-rotating nozzle creates a continuous flow of droplets at the chamber wall by impact momentum effects. The aim of this study was to design and test a new self-rotating nozzle to improve the condensation rate in the flash-purifier. The device investigated employed a self-rotating nozzle of innovative design. The new system was constructed successfully and tested under conditions in which the vacuum and feed-water pressures, and the temperature were varied to maximize the condensation rate. Factorial design methodology showed that vacuum pressure was the most influential variable for condensation rate. The highest condensation rate achieved was 0.0748 ml/s, obtained from a combination of 2.0 bar-g feed-water pressure, vacuum pressure 0.3 bar-a and feed-water temperature 60 °C. Previous studies involved an electric rotating nozzle that generated 0.061 ml/s, but this study proved the efficiency of the self-rotating nozzle by producing a higher condensation rate.

Key words: condensation rate, flashing chamber, flash purification, rotating nozzle, self-rotating nozzle

Highlights

- Flash purification.
- Self-rotating nozzle.
- Condensation and evaporation rate.

INTRODUCTION

The flash purification system tested in this study was based on a hybrid system developed by Bai (2011), Date *et al.* (2015), and Zhao *et al.* (2009), for combined desalination and power generation (CDP). The main objective of this study was to develop an efficient system that used hot geothermal brine as a working fluid to generate electricity and produce clean water simultaneously. Flash purification is similar to flash desalination, being distinguished only by the working fluid – seawater in desalination and wastewater for purification. Flash purification is a vacuum process for separating solids from wastewater. Wastewater is pumped into the flash chamber, where it is flash-evaporated and then condensed to produce clean water. Flashing uses a rotating nozzle to distribute water droplets evenly inside the flash chamber and produce a good condensation rate compared to a stationary nozzle.

Desalination and purification technology developed by Sonawan *et al.* (2015) used a rotating nozzle driven by a DC electric motor to distribute droplets in a flashing chamber. Rotating nozzles yield higher condensation rates than stationary nozzles and using a lower nozzle rotation speed gives even better results (Sonawan & Riki 2016). A rotating nozzle was used again for this study but its design differed from those used previously. For this study, the rotary force came from the momentum of the water leaving the nozzle. This self-rotating nozzle produced a higher condensation rate than the rotating nozzle used previously.

METHODS

The purpose of flash-purification is to produce clean water (condensate) via evaporation and subsequent condensation in a flashing chamber. A water jet from the nozzle hits the flashing chamber wall and splits into droplets, which evaporate and are then condensed. The evaporation rate affects the condensation rate greatly.

Theoretical approach and hypothesis

The water from the self-rotating nozzle hits the chamber wall and breaks into droplets that evaporate quickly. Figure 1 shows that the water jet hits the chamber wall and is deflected as a spray of fine droplets at angle α. The coverage angles depend on the rotor and flashing chamber radii (Equation (1)). The greater the rotor's radius, the smaller the coverage angle, reducing the evaporation rate because fewer droplets are produced.

$$\alpha = 90^{\circ} - \arcsin\frac{r}{R} \tag{1}$$

The feed-water's impact on the chamber wall produces droplets that evaporate quickly. Thus, the water's velocity as it leaves the nozzle, which is a function of the water pressure, has a strong effect on the number of droplets produced. The faster the droplets evaporate in the chamber, the greater the condensation rate and the strong impact on the chamber wall helps droplet formation. High feed-water pressure results in high water velocity, generating great momentum when colliding with the wall and maximizing droplet spray.

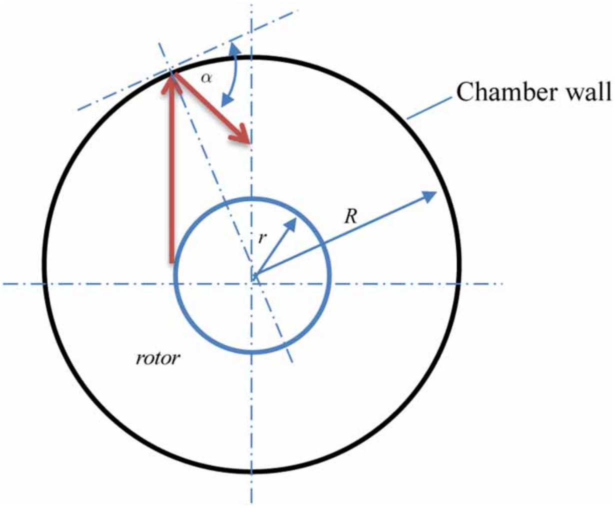

Figure 1 | Flashing chamber, illustrating the coverage angle.

Variables

The condensation rate is influenced by many factors, but in this study only three variables were tested – vacuum (P_v), feed-water pressure (P_m), and feed-water temperature (T_m). The test system comprised a flashing chamber, rotor and nozzle, plus measurement instrumentation.

The trial setup is shown in Figure 2. The main component is the flashing chamber (2) containing the self-rotating nozzle (3–4). The nozzle has a double role as feed-water sprayer and, due to its momentum, mechanical power generator. The feed-water passes through a gas heater (5) to raise its temperature and on to a pump (6). Before the feed-water was pumped through the nozzle, the air inside the flash chamber was removed by a vacuum pump (7). This lowered the feed-water's boiling point, increasing the evaporation rate and yielding a larger vapor fraction.

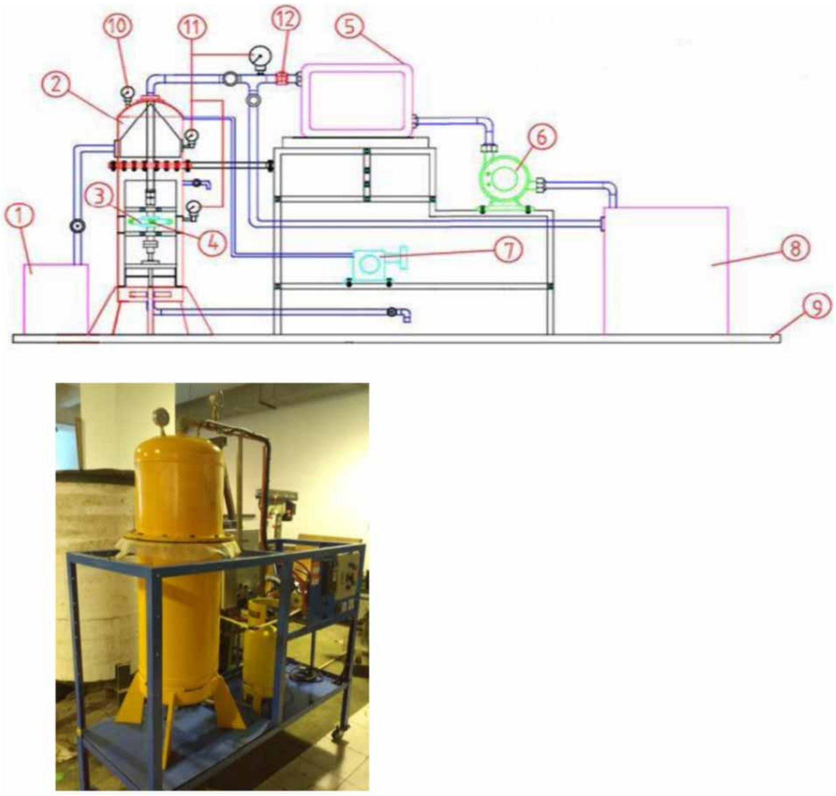

Figure 2 | Flash-purification apparatus.

The feed-water temperature and pressure, and the vacuum pressure, were tested at both low and high levels (Table 1).

Table 1 | Variables tested

Level	Feed-water temperature T_m, (°C)	Feed-water pressure P_m, (bar-g)	Vacuum pressure P_v, (bar-a)
Low	60	1.5	0.3
High	70	2.0	0.4

To maintain efficiency, the feed-water temperature was set as low as possible to reduce the heating energy needed. Energy conservation was also the main consideration when choosing feed-water pressure. A centrifugal pump was used to produce high feed-water velocity from the nozzles. Higher pressure produces higher velocity, but in this study, the pressure was limited to 2.0 bar-g to keep power consumption down. Flash purification was performed in a vacuum to increase the evaporation rate and the vacuum was set to 0.3 bar-a (absolute) maximum, again to keep power consumption down commensurate with high efficiency.

A design factorial 2^3 methodology was used and the configurations are shown in Table 2. It was more difficult to control feed-water temperature to the set level than to control pressure, so the first experiments were conducted at 60 °C feed-water temperature (configurations 1, 3, 5, and 7) followed by those at 70 °C (2, 4, 6, and 8). Experiments were repeated four or five times for each configuration to control for measurement uncertainty. The experimental responses or output variables were condensate volume and steady-state time, and both were used to calculate the condensation rate.

Table 2 | Configuration for condensation rate measurement

Configuration	Feed-water temperature (°C)	Feed-water pressure (bar-g)	Vacuum pressure (bar-a)	Condensation rate (ml/s)
1	60	1.5	0.3	Measured in experiments
2	70	1.5	0.3	
3	60	2.0	0.3	
4	70	2.0	0.3	
5	60	1.5	0.4	
6	70	1.5	0.4	
7	60	2.0	0.4	
8	70	2.0	0.4	

RESULTS AND DISCUSSION

The temperature and feed-water flow rate measurements were used to ensure that steady-state had been achieved. The flashing and feed-water temperatures, and the flow rate measurements, are presented in Figure 3.

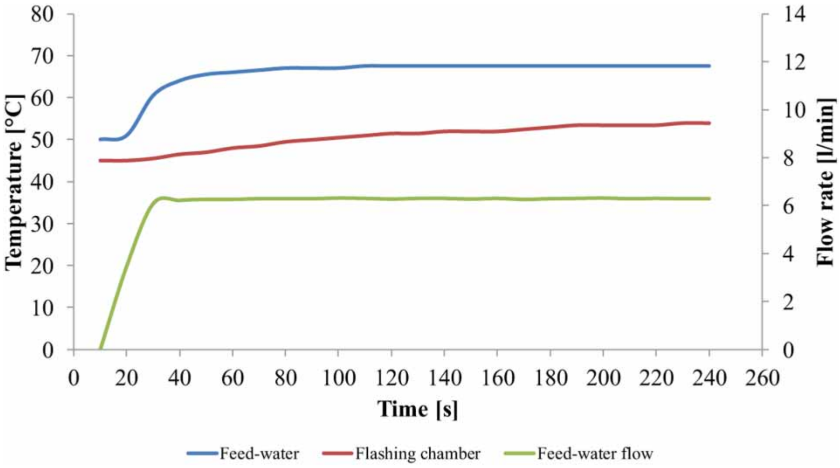

Figure 3 | Change in temperature and flow with time (feed-water temperature 70 °C, feed-water pressure 2.0 bar-g, vacuum pressure 0.4 bar-a).

The curve trends were similar for all experiment configurations. The vapor temperature in the flashing chamber began to reach equilibrium after about one minute but this was not true of the feed-water temperature. The difficulty in reaching the set temperature was a constraint and a new method of maintaining constant feed-water temperature throughout the experiment had to be considered. Increasing the water flow rate allows faster attainment of equilibrium and, generally, water flow adjustments were maintained and the steady-state time could be determined accurately (Figure 3). The results from the different experimental designs are shown in Table 2. The condensation rate averages were calculated from each experimental configuration, with a margin of error at 95% confidence level requirement.

Figure 4 shows the experimental results at vacuum pressures of 0.3 and 0.4 bar-a – all of those accepted were within the range of the margin of error. For example, one of the data points from experiment #3 – feed-water temperature 60 °C, pressure 1.5 bar-g and vacuum pressure 0.3 bar-a – was outside the margin of error and removed from the dataset, leaving the remaining four to be averaged. This method was applied consistently to all configurations at different combinations of temperature and pressure (Table 3). Changes in feed-water temperature from 60 to 70 °C at the same feed-water pressure do not produce consistent changes in condensation rate; sometimes it goes up and sometimes down. Likewise, changes in feed-water pressure from 1.5 to 2.0 bar-g at the same feed-water temperature do not produce consistent condensation rate changes. The condensation rate varied with no consistent trend, so the data were analyzed further using Yates' algorithm (Table 4) (Box *et al.* 1978).

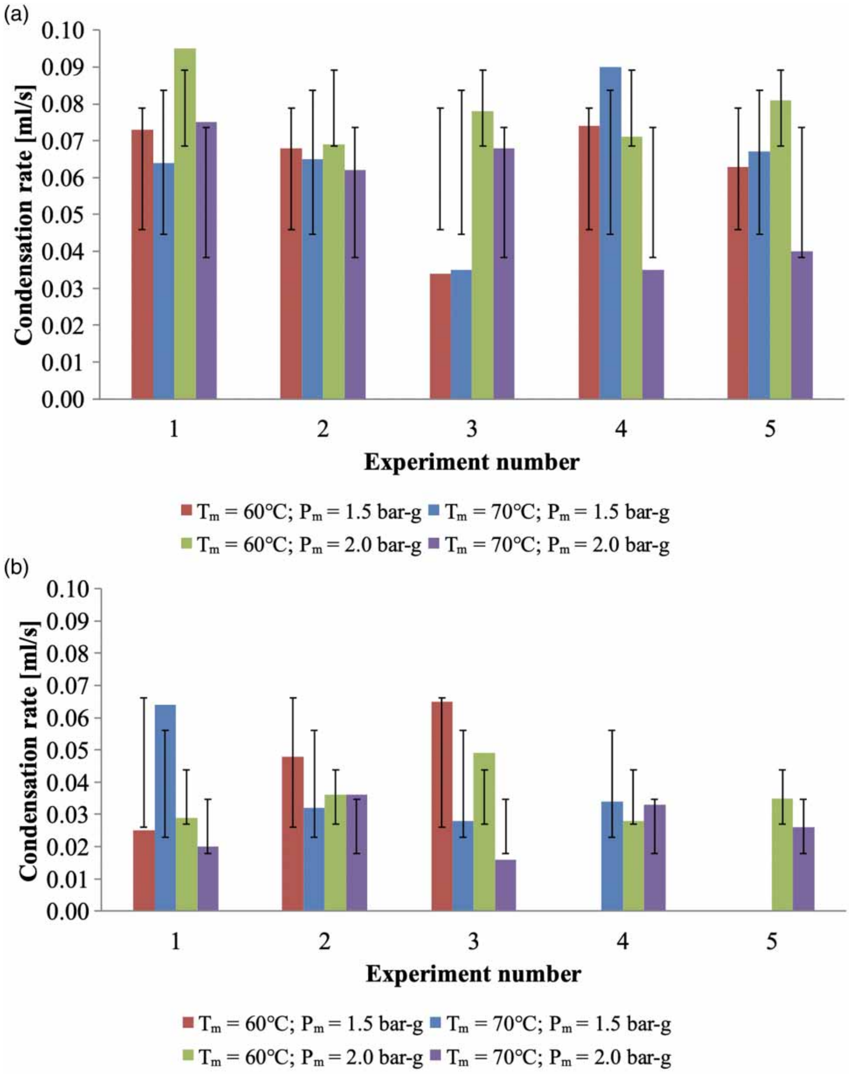

Figure 4 | Condensation rates at vacuum pressures of (a) 0.3 bar-a, and (b) 0.4 bar-a.

Table 3 | Mean condensation rates from the various configurations

Configuration	Feed-water temperature (°C)	Feed-water pressure (bar-g)	Flashing pressure (bar-a)	Condensation rate (ml/s)
1	60	1.5	0.3	0.0695
2	70	1.5	0.3	0.0653
3	60	2.0	0.3	0.0748
4	70	2.0	0.3	0.0567
5	60	1.5	0.4	0.0565
6	70	1.5	0.4	0.0313
7	60	2.0	0.4	0.0320
8	70	2.0	0.4	0.0263

Table 4 | Data calculations using the Yates algorithm

Average condensation rate (ml/s)	1st	Counts 2nd	3rd	Divider	Results	Remarks
0.0695	0.1348	0.2663	0.4124	8	0.0515	Average
0.0653	0.1315	0.1461	−0.0532	4	−0.0133	T_m
0.0748	0.0878	−0.0223	−0.0328	4	−0.0082	P_m
0.0567	0.0583	−0.0309	0.0056	4	0.0014	T_m-P_m
0.0565	−0.0042	−0.0033	−0.1202	4	−0.0301	P_v
0.0313	−0.0181	−0.0295	−0.0086	4	−0.0022	T_m-P_v
0.0320	−0.0252	−0.0139	−0.0262	4	−0.0066	P_m-P_v
0.0263	−0.0057	0.0195	0.0334	4	0.0084	T_m-P_m-P_v

The data in Table 3 were calculated using Yates algorithm to obtain variables that affect the condensation rate and the results shown in Table 4. Higher values indicate greater effects. The values in the results column of Table 4 were calculated from the 3rd value (column 4) divided by the divider and their association is given in the remarks column (7). The value 0.0515 – row 1, column 6 – is the average, the value −0.0133 – row 2, column 6 – with T_m, and so on.

The average condensation rate was 0.0515 ml/s (Table 4). Of the three variables tested, vacuum pressure (P_v) had the most influence on condensation rate, which increased 0.0301 ml/s when P_v was raised from 0.4 to 0.3 bar-a; that is, the condensation rate increase from 0.0320 to 0.0621 ml/s was within the range limit 0.0301 ml/s. The higher vacuum pressure increased the condensation rate by increasing the vapor fraction in the flashing chamber because water droplets hitting the chamber walls with sufficient force raise the chamber's vapor content, increasing evaporation.

Feed-water pressure (P_m) was the least important variable in flashing. Lowering it from 2.0 to 1.5 bar-g increased the condensation rate by only 0.0082 ml/s. For example, the condensation rate increase from 0.0567 to 0.0649 ml/s was within the range limit 0.0082 ml/s. Compared to changes in P_v, changes in P_m have a smaller effect. The Yates algorithm makes it possible to analyze the condensation rate through the effects of a single variable – for example, P_m, P_v or T_m – as well as by the interaction between variables. Thus, if the feed-water temperature and pressure were changed simultaneously (T_m – P_m), the condensation rate increased by 0.0014 ml/s. A higher rate of 0.0066 ml/s might be obtained if the feed-water pressure was changed simultaneously with the vacuum pressure (P_m – P_v). Desalination by flash purification could be increased if the vacuum pressure was set as high as possible, as shown in the thermodynamic pressure – enthalpy diagram (Figure 6).

To improve the analysis, a new variable was introduced, the difference in pressure between the feed-water and vacuum (P_m – P_v), which indicates the pressure differential within the nozzle. The correlation between pressure difference and feed-water temperature in relation to condensation rate is shown in Figure 5. The condensation rate was higher at a feed-water temperature of 60 than 70 °C, which is contrary to the throttling concept evaluated on the thermodynamic pressure-enthalpy diagram. The diagram in Figure 6 shows two throttling processes (iso-enthalpy) with different feed-water temperatures and vacuum pressures. The iso-enthalpy process at 60 °C yields a smaller vapor fraction – the ratio of vapor quantity to the total amount of vapor and liquid in the chamber – than at 70 °C. Higher feed-water temperature at the same feed-water pressure might produce a higher vapor fraction – that is, a higher vapor proportion to condensation rate.

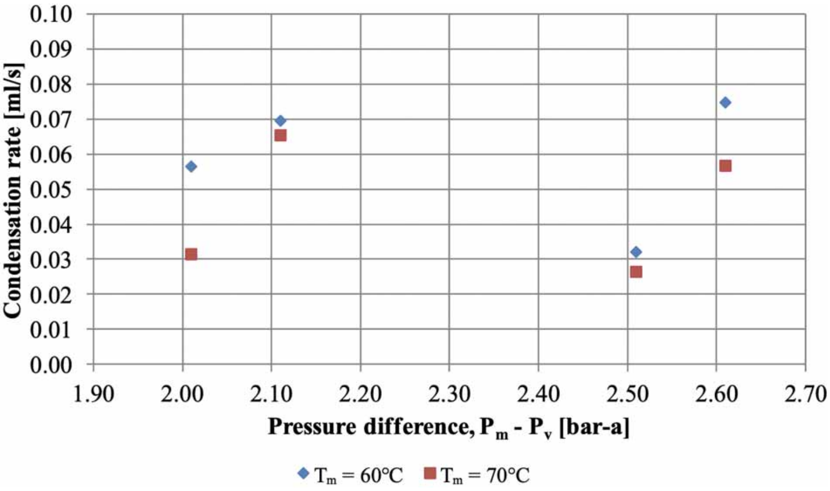

Figure 5 | Influence of Feed-water Pressure and Temperature on Condensation Rate.

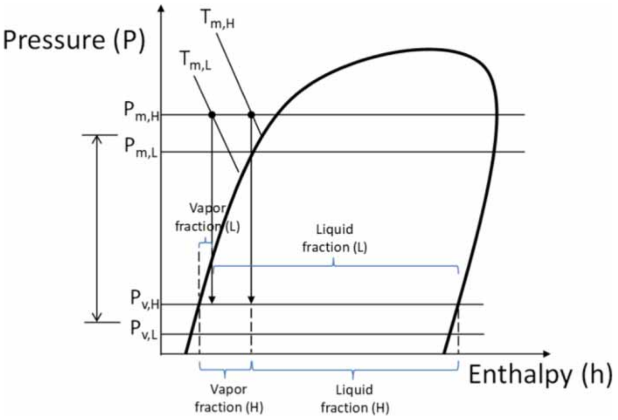

Figure 6 | Pressure – enthalpy diagram.

As it is affected by the feed-water temperature, a higher pressure difference might produce a higher vapor fraction and condensation rate, as well. The higher differential could be achieved by increasing either the feed-water or vacuum pressure. Figure 5 shows that the entire higher pressure differential is proportional to the higher condensation rate. The higher pressure differential leads to the production of finer droplets (vapor), encouraging faster evaporation in the low pressure environment.

In previous work, the highest condensation rate achieved using a rotating nozzle in flash purification was about 0.061 ml/s (Sonawan & Riki 2016). In that study, the condensation rate increased from 0.0143 ml/s at zero rpm to 0.061 ml/s at 15 rpm, then decreased to 0.0195 ml/s at 34 rpm (Figure 7). In this study, using a self-rotating nozzle, the maximum condensation rate achieved

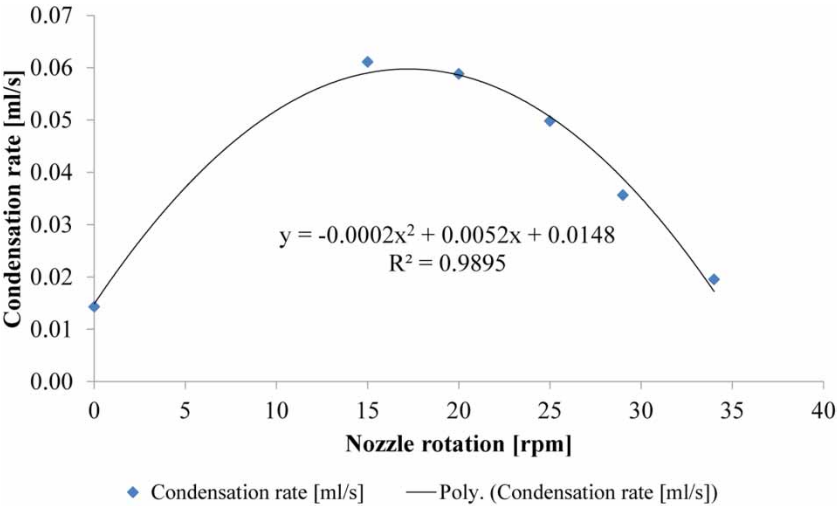

Figure 7 | Flash purification condensation rate using a rotating nozzle.

was 0.0748 ml/s – that is, it was more efficient. The self-rotating nozzle was cheaper to manufacture and operate than the electrically operated version. Its rotation speed can be controlled by adjusting the feed-water pressure to obtain the optimum condensation rate.

CONCLUDING REMARKS

1. A flash purification system using a self-rotating nozzle has been developed.
2. The variable with the greatest effect on condensation rate was vacuum pressure. A vacuum pressure of 0.3 bar-a produced a higher condensation rate than 0.4 bar-a.
3. The highest condensation rate of 0.0748 ml/s was obtained operating at feed-water pressure and temperature 2.0 bar-g and 60 °C, and vacuum pressure 0.3 bar-a.

REFERENCES

Bai, F. 2011 *A Novel System for Combined Power Generation and Water Desalination Using Renewable Energy*.

Box, G. E., Hunter, W. G. & Hunter, J. S. 1978 *Statistics for Experimenters*. John Wiley and Sons, New York, NY.

Date, A., Khaghani, A., Andrews, J. & Akbarzadeh, A. 2015 Performance of a rotating two-phase turbine for combined power generation and desalination. *Applied Thermal Engineering* **76**, 9–17.

Sonawan, H. & Riki 2016 Pengoptimalan Kecepatan Putar Nosel pada Proses Flashing Purification yang Menggunakan Nosel Berputar (Optimizing the rotational speed of the rotating nozzle in the flashing purification). Seminar Nasional ke-3 (The 3rd National Seminar), 2016 Makassar. Teknik Mesin (Mechanical Engineering Dept.), Universitas Hasanuddin.

Sonawan, H., Abdurrachim, Tandian, N. P. & Yuwono, S. 2015 Studi Eksperimen Proses Flashing Dari Nosel Berputar di Dalam Lingkungan Vakum. *Prosiding SENATEK 2015* **1**, 301–305.

Zhao, Y., Akbarzadeh, A. & Andrews, J. 2009 Simultaneous desalination and power generation using solar energy. *Renewable Energy* **34**, 401–408.